



# A Method for Genotyping Murine Arylamine *N*-Acetyltransferase Type 2 (NAT2): A Gene Expressed in Preimplantation Embryonic Stem Cells Encoding an Enzyme Acetylating the Folate Catabolite *p*-Aminobenzoylglutamate

Mark Payton, Valerie Smelt, Anna Upton and Edith Sim\*

UNIVERSITY DEPARTMENT OF PHARMACOLOGY, UNIVERSITY OF OXFORD, MANSFIELD ROAD, OXFORD, U.K.

**ABSTRACT.** Mice have three arylamine *N*-acetyltransferase (NAT) isoenzymes (NAT1, NAT2, and NAT3) of which NAT2 is known to be polymorphic. Humans have two polymorphic isoenzymes, NAT1 and NAT2. The isoenzymes mouse NAT1 and human NAT2 are expressed predominantly in the liver and intestine and are involved in drug and xenobiotic metabolism. Mouse NAT2 and human NAT1 have a widespread tissue distribution and the folate catabolite *p*-aminobenzoylglutamate (*p*AB-Glu) has been proposed as a candidate endogenous substrate. All mice have detectable NAT2 activity, although inbred mouse strains have either a fast or slow acetylator phenotype conferred by the presence of either NAT2\*8 (fast) or NAT2\*9 (slow) alleles at the NAT2 locus. In this report, we describe a simple method for distinguishing these murine alleles by polymerase chain reaction followed by restriction fragment length polymorphism analysis. We compared the tissue distribution of the acetylation activity found in both fast (C57BL/6J) and slow (A/J) acetylating strains of mice using *p*AB-Glu and *p*-aminobenzoic acid as probe substrates. It has previously been demonstrated that murine NAT2 is expressed in the neural tube prior to closure (Stanley L, Copp A, Rolls S, Smelt V, Perry VH and Sim E, *Teratology* **58**: 174–182, 1998). We demonstrate here that murine NAT2 is expressed in preimplantation embryonic stem cells. Murine NAT2 is likely to be expressed prior to neurulation and this may be important in view of the protective role of folate in neural tube development. *BIOCHEM PHARMACOL* **58**:5:779–785, 1999. © 1999 Elsevier Science Inc.

**KEY WORDS.** mouse; NAT; genotyping; folate; embryonic stem cells

Acetylation of aromatic amines and hydrazines by NAT<sup>†</sup> (EC 2.3.1.5.) has been shown to be an important route in their metabolism (for review, see [1]). NATs catalyse the acetyl-CoA-dependent *N*-acetylation of these compounds, resulting in their detoxification. NAT can also activate potential DNA adduct-forming compounds by catalysing the *O*-acetylation of arylhydroxylamines [2, 3]. Three functional murine NAT isoenzymes (NAT1, NAT2, and NAT3) [4, 5], and two human isoenzymes (NAT1 and NAT2) [6, 7] have been identified. Murine NAT2 [8, 9] and both human isoenzymes are known to be polymorphic [10–13]. It has been demonstrated that polymorphisms in the human NAT2 gene affect susceptibility to environmentally induced bladder cancer, such that the slow acetylator

phenotype confers a greater risk [14, 15]. It has also been suggested that polymorphisms at human NAT1 may affect cancer susceptibility [16], though this has been disputed [17]. Furthermore, it has been shown that mice of the slow acetylator type are more susceptible to carcinogenesis [18].

Together with the ability to catalyse the acetylation of carcinogens, NAT isoenzymes also act on a range of non-carcinogenic compounds, including hydrazines and arylamines [19–22]. Mouse isoenzymes NAT1 and NAT2 demonstrate distinct substrate profiles, metabolising isoniazid and *p*ABA, respectively; they have shared specificity for 2-aminofluorene [23, 24]. These substrate profiles have been exploited to identify the tissue distribution of murine NAT1 and NAT2 [25]. Studies have also been supplemented by immunohistochemical analysis using antipeptide antibodies which specifically recognise murine NAT2 [26]. As yet, no probe substrate has been identified for murine NAT3 [4, 24, 27]. Mouse NAT1 and human NAT2 are found predominantly in the liver, whereas mouse NAT2, like human NAT1, is found in most tissues [26]. On the basis of the similarity of their tissue distribution and substrate specificities, human NAT1 and mouse NAT2

\* Corresponding author: Prof. Edith Sim, University Department of Pharmacology, University of Oxford, Mansfield Road, Oxford, U.K. Tel. +441865 271596; FAX +441865 271853; E-mail: esim@worf.molbiol.ox.ac.uk

<sup>†</sup> Abbreviations: ApAB-Glu, acetyl *para*-aminobenzoylglutamate; gDNA, genomic DNA; NAT, arylamine *N*-acetyltransferase; NTD, neural tube defects; *p*ABA, *para*-aminobenzoic acid; *p*AB-Glu, *para*-aminobenzoylglutamate; and PCR, polymerase chain reaction.

Received 12 December 1998; accepted 25 February 1999.

TABLE 1. Amino acid comparison of human and mouse NAT isoenzymes

	Human (NAT1)	Mouse (NAT1)	Mouse (NAT2)	Mouse (NAT3)
Human (NAT1)	—	[85.8]	<u>[90.3]</u>	[80.7]
Mouse (NAT1)	74.8	—	[90]	[82]
Mouse (NAT2)	<u>82</u>	81.7	—	[83.4]
Mouse (NAT3)	68.2	67.6	73.4	—

Sequence similarity is depicted in square brackets and identity without brackets. Comparisons between human NAT1 and mouse NAT2 are underlined. NAT enzyme isoform is shown in curved brackets below species name.

have been proposed to have a similar role in both species. A comparison at the amino acid level of human NAT1 with the mouse NAT isoenzymes demonstrates a higher level of similarity to mouse NAT2 than to the two other mouse isoenzymes (Table 1). There is an identity of 82% and a similarity of 90.3% between human NAT1 and mouse NAT2. In addition, studies of heterologously expressed murine enzymes have demonstrated that recombinant mouse NAT2 could catalyse the acetylation of the human NAT1 probe substrate *p*ABA [8, 23, 26]. It has been proposed [26] and subsequently demonstrated [24] that the folate catabolite *p*AB-Glu is a substrate of murine NAT2. The compound *p*AB-Glu has previously been described as a likely substrate of human NAT1 [21, 28].

Folate catabolism in humans and rodents involves the enzymatic reduction of the folate molecule to tetrahydrofolate followed by cleavage, which may be spontaneous, at the C9-N10 position to yield the pteridine moiety and *p*AB-Glu [29]. Radiolabelled folate has been used to show that the main metabolite excreted in the urine of rodents is the acetylated form of *p*AB-Glu, *Ap*AB-Glu [30]. Human NAT1 can *N*-acetylate *p*AB-Glu [21, 28] and may play a role in removing biologically inactive metabolites from the folate cycle. This is an important finding in the light of recent evidence on human NAT1 polymorphisms [10–12]. It has been shown that during pregnancy there is an increased catabolism of folate resulting in an elevated excretion of *Ap*AB-Glu in rodents [31] and humans [32]. This may explain the requirement for folate supplementation during pregnancy which is known to protect against NTD in humans [33]. Studies have linked certain developmental disorders associated with neural tube closure, such as cleft lip and cleft lip and palate, to the NAT2 locus in the mouse [34, 35].

To investigate the potential role of NAT in folate metabolism, it is essential to have a useful model. Mice provide a good model in that there are inbred strains of known NAT phenotype [23]. We have established a simple method for genotyping NAT2 in mouse strains and have also investigated the relationship between mouse NAT2 activity, determined using *p*ABA as substrate, and the ability to metabolise the folate catabolite *p*AB-Glu. In view of the protective role of folate in neural tube defects, we

have investigated whether NAT might be expressed prior to neurulation. It has been shown previously using immunohistochemistry that NAT2 is present in the neural tube in 9.5-day mouse embryos [36], and we demonstrate here that the NAT2 gene is transcribed in embryonic stem cells, indicating that it is present prior to implantation.

## MATERIALS AND METHODS

### Chemicals and Animals

All chemicals were obtained from Sigma Chemical Company and molecular biology reagents were from Promega, unless otherwise stated. All mouse strains were obtained from Park Farm, Oxford except for CBA/6J, which were obtained from the Oxford University Biomedical Unit.

### Genomic DNA Isolation

gDNA was extracted from mouse tissue homogenates as previously described for preparation of gDNA from human blood [15]. Mouse embryonic stem cells (ES 129 ola) were kindly donated by Dr. Frances Brook (Department of Zoology, University of Oxford) and were also used for the preparation of gDNA, as before [15].

### PCR and PCR–Restriction Fragment Length Polymorphism (RFLP) Analysis

As the open reading frame of NAT is intronless, all PCR amplifications were from gDNA. PCR amplification was carried out using high-fidelity pfu DNA polymerase (error rate of  $1.3 \times 10^{-6}$ ; Stratagene) for sequence analysis. The open reading frame of murine NAT2 was amplified using the primers 5'MNAT2/1 (5'-ATGGACATCGAAGCGTACTTTG-3') and 3'MNAT2/910 (5'-TTCCAAGTACATGGAAGGACACC-3'), in which the underlined number relates to the point of primer attachment (1 represents the adenosine of the start codon ATG). Primers were annealed at 58° for 30 sec and product elongation was at 72° for 2 min to yield a 910 bp cDNA product. PCR reactions were cycled for 15 times to minimise the incorporation of errors. Specific murine NAT2 primers were used for PCR–RFLP analysis and amplification was performed

using Taq DNA polymerase (Promega). cDNA was amplified by PCR using the murine *NAT2* specific primers 5'MNAT2/278 (5'-GTCTTTAACTCCAGCC-3') and 3'MNAT2/409 (5'-ATTCCAGAGGCTCCCAC-3'), in which the underlined number relates to the point of primer attachment (1 represents the adenosine of the start codon ATG). Primers were annealed at 54° for 30 sec and product elongation was at 72° for 30 sec to yield a 128 bp cDNA product. The PCR product was digested with *Tru91* (*MseI*) at 65° for 90 min. Products were analysed by electrophoresis on a 3% MetaPhor (Flowgen)/1% agarose (Boehringer) gel. The gene coding for murine  $\beta$ -actin [37] was amplified by PCR across introns II, III, and IV, using Taq polymerase and the primers actin-sense 5'-GGATGACGATATCGCTGC-3' and actin-antisense 5'-GTGGTACCACCAGACAGCA-3'. Primers were annealed at 58° for 30 sec and product elongation was for 2 min. Product sizes from gDNA and cDNA were predicted to be 1580 bp and 910 bp, respectively.

### Sequencing of Murine *NAT2*

PCR amplification from gDNA was performed using high-fidelity proofreading pfu DNA polymerase (Stratagene). Products were 3' tagged with dATP, cloned into the vector pGEMT (Promega), and analysed with M13 forward and reverse primers using an ABI 377 automated sequencer (The Advanced Biotechnology Centre, London).

### Detection of mRNA in Embryonic Stem Cells

Total RNA was extracted from embryonic stem cells, using Tri-Reagent™ (Sigma), and was used as a template for cDNA synthesis by reverse transcriptase-PCR. Amplification by PCR of murine *NAT2* and the gene encoding for murine  $\beta$ -actin was then performed on cDNA using the specific primers described above.

### Enzymic Assays

Mice were killed by cervical dislocation. Blood was collected in 10 mM potassium phosphate pH 7.5, 1.15% (w/v) potassium chloride, 5 mM EDTA after decapitation. Isolated tissues were either used directly for cytosol preparation or snap-frozen in liquid N<sub>2</sub>. For cytosol preparation, tissues were prepared in three times their mass of potassium-EDTA buffer (10 mM potassium phosphate pH 7.5, 1.15% (w/v) potassium chloride, 1 mM EDTA, 1 mM dithiothreitol and 0.5 mM pepabloc (protease inhibitor; S. Black) and homogenised on ice with three bursts of 2 min using a tissue grinder (Janke and Kunkel™, labortechnik Ultra-Turrax T25). The homogenate was centrifuged (14,500 g for 20 min at 4°) and the supernatant collected. This supernatant was subjected to a further centrifugation (100,000 g for 1 hr at 4°) to pellet the microsomal fraction. The cytosol in the supernatant was snap-frozen and stored in liquid N<sub>2</sub>. Murine *NAT2* activities were determined

Human <i>NAT1</i> *4	ACT	CCA	GCC	AAA	AAA	TAC	AGC
	T	P	A	K	K	Y	S
Mouse <i>NAT2</i> *8	ACT	CCA	GCC	AAT	AAG	TAC	AGC
	T	P	A	<b>N</b>	K	Y	S
				<u>Tru91</u>			
Mouse <i>NAT2</i> *9	ACT	CCA	GCC	<b>ATT</b>	<b>AAG</b>	TAC	AGC
	T	P	A	<b>I</b>	K	Y	S

FIG. 1. Known polymorphisms within the murine *NAT2* open reading frame compared to wild-type human *NAT1*. A unique *Tru91* restriction site is shown (T/TAA) which distinguishes murine *NAT2*\*8 from *NAT2*\*9. Nucleotides and amino acids are represented as single letter codes and are in bold face if different from the most common human allotype, *NAT1*\*4.

using pABA as a substrate [26]. *N*-Acetylation of pAB-Glu was determined by HPLC (Waters 484/600E) with UV detection at 266 nm using a modified method to that previously described [38]. Arylamine substrates were used at a concentration of 0.22 mM, with acetyl-CoA at 0.44 mM.

## RESULTS

### Murine *NAT2* Genotype Determination and Acetylation Phenotype

Open reading frames representing murine *NAT2* were sequenced from mouse strains A/J, C57BL/6J, 129 ola embryonic stem cells, CBA/B6, and Balb/c. The mouse sequences were identical except at nucleotide position 296. At this point, an A<sup>296</sup>T mutation results in the creation of a *Tru91* restriction site and an amino acid substitution of ASN<sup>99</sup>ILE (Fig. 1). This point mutation creates a slow acetylation phenotype, *NAT2*\*9, from a fast acetylation phenotype, *NAT2*\*8 [8]. The sequence surrounding this point mutation is highly conserved when compared to the most common allele of human *NAT1* [6, 7], which has a LYS in place of the murine ASN/ILE (*NAT2*\*8/*NAT2*\*9). A 128 bp fragment was PCR-amplified from murine gDNA using specific primers for murine *NAT2* (5'MNAT2/1 and 3'MNAT2/910). Digestion with *Tru91* revealed the presence of a smaller band of 112 bp, characteristic for *NAT2*\*9, in the A/J mouse (Fig. 2, lane 7). All other products remained the same size as the undigested product, 128 bp, characteristic of *NAT2*\*8 (Fig. 2, lanes 2–6 and 8–11). Genotypes as described in Fig. 2 in comparison with phenotypes for different mouse strains are shown (Table 2). There is a good correlation of genotype and phenotype, and it is proposed that the 129 ola strain of embryonic stem cells is derived from a fast acetylating strain of mice.

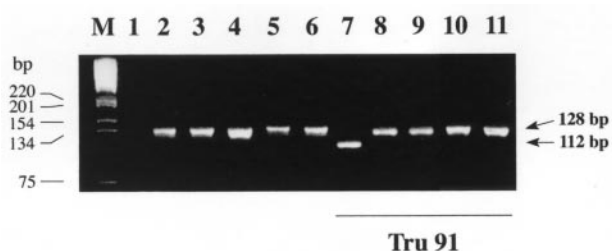


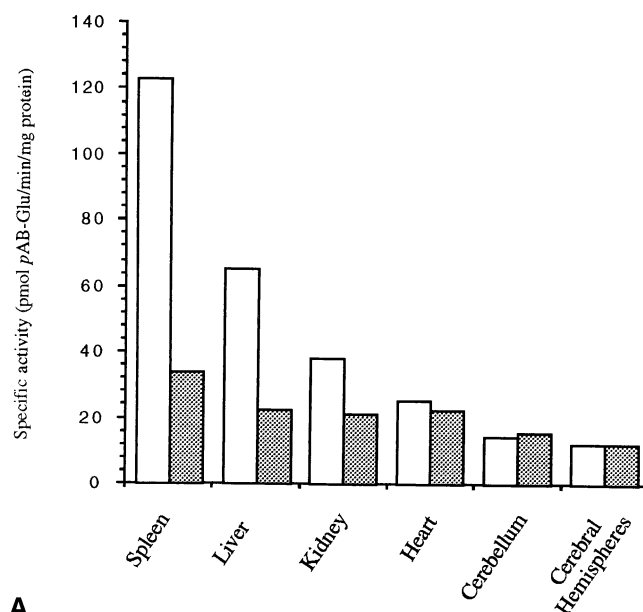
FIG. 2. Gel electrophoresis of murine NAT2 PCR-amplified products before and after restriction digestion with *Tru91*. Amplification of gDNA results in a fragment of 128 bp which is digested to 112 bp for NAT2\*9, and remains at 128 bp for NAT2\*8. Lane M represents a 1 kb marker (GIBCO BRL). Lane 1 is a blank containing no gDNA, lanes 2 to 6 are PCR products, prior to digestion, amplified from gDNA isolated from A/J, C57BL/6J, 129 ola embryonic stem cells, CBA/B6, and Balb/c respectively. Lanes 7 to 11 are PCR products digested with *Tru91*.

#### N-Acetylation of *pAB-Glu* and *pABA* Using Mouse Tissue Cytosols

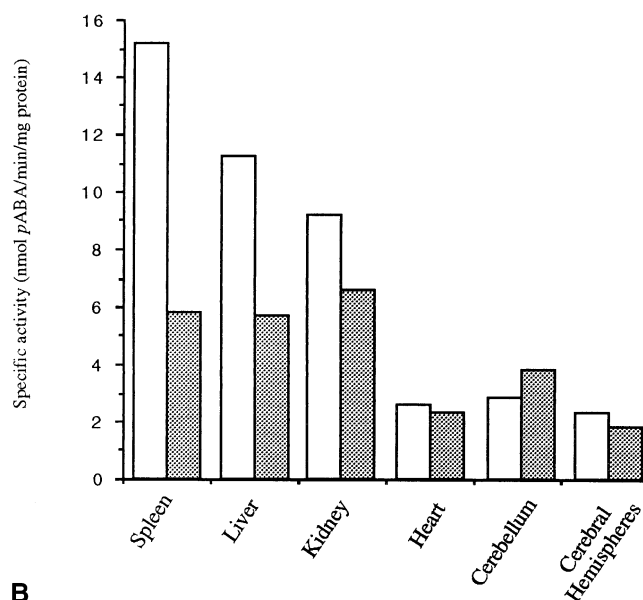
Acetylation of *pAB-Glu* (Fig. 3a) in both fast and slow acetylating mouse strains followed a similar pattern to that found when using *pABA* as substrate (Fig. 3b). With both substrates, a difference in the specific activity of acetylation was observed between the two strains of mice for the tissues liver, kidney and spleen. There was a less marked difference between the specific activities of the two strains for heart tissue. Two areas of the brain were investigated and were found to have a lower, but measurable, specific activity compared with the other tissues investigated using *pABA* and *pAB-Glu* as substrates. These results indicate a low level of murine NAT2 in the brain and are in agreement with other studies [25], including immunohistochemical analysis which demonstrated specific recognition of murine NAT2 within the Purkinje cells of the cerebellum of mice [36].

#### Transcription in Embryonic Stem Cells

In order to determine whether murine NAT2 was being transcribed in embryonic stem cells, mRNA was prepared and cDNA was made by reverse transcription. PCR amplification was performed using two sets of primers for murine NAT2 and  $\beta$ -actin, as described in Methods. The primers for murine NAT2 will generate a product of 910 nucleo-



A



B

FIG. 3. Comparison of acetylation of (A) *p*-aminobenzoylglutamate and (B) *p*-aminobenzoic acid as substrates with cytosols of different tissues isolated from fast (C57BL/6J) and slow (A/J) acetylating strains of mice. The white columns represent C57BL/6J mice and the shaded columns represent A/J mice. An average of two independent determinants are shown, these values being within a 5 percent error.

TABLE 2. Determined genotype and phenotype for different mouse strains

Mouse strain	Genotype	Phenotype	Reference
A/J	NAT2*9	Slow	Tannen & Weber, 1980
C57BL/6J	NAT2*8	Fast	Tannen & Weber, 1980
129 ola embryonic stem cell	NAT2*8	Fast	*
CBA/B6	NAT2*8	Fast	†
Balb/c	NAT2*8	Fast	Kelly and Sim, 1994

\* Determined from genotype.

† Determined by comparison of specific activity of *pABA* acetylation in blood. A/J; 0.071 nmol. min<sup>-1</sup> mg protein<sup>-1</sup>. CBA/B6; 2.17 nmol. min<sup>-1</sup> mg protein<sup>-1</sup>.



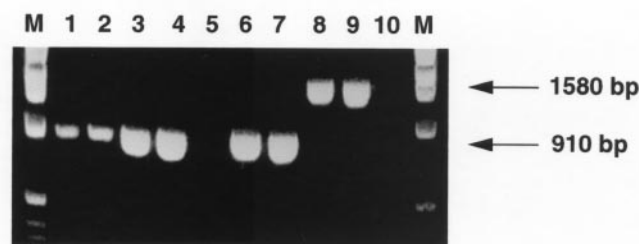


FIG. 4. PCR amplification from cDNA and genomic DNA isolated from embryonic stem cells using specific primers for murine NAT2 and the gene coding for murine  $\beta$ -actin. PCR products using primers specific for murine NAT2 (lanes 1–5) and part of the gene encoding for  $\beta$ -actin (lanes 6–10) are shown. Lane M represents a DNA ladder (GIBCO BRL). Lanes 1, 2, 6, and 7 represent amplification from cDNA. Lanes 3, 4, 8, and 9 represent amplification from gDNA. Lanes 5 and 10 are blanks which contain no template DNA.

tides from both cDNA and gDNA. The primers specific for the mouse  $\beta$ -actin gene will generate products of 1580 and 910 nucleotides from mouse gDNA and cDNA, respectively. The results shown (Fig. 4) clearly demonstrate that the cDNA preparation contains no gDNA as indicated by the presence of a 910 bp product only when primers specific for the murine  $\beta$ -actin gene were used. There is no detectable contamination of cDNA by gDNA, since a control amplification from gDNA using the same primers indicates the presence of a product at 1580 bp, a result of the introns within the  $\beta$ -actin gene [37]. Thus, it can be concluded that under the conditions used, amplification by PCR of murine NAT2 is due to the presence of transcribed RNA (cDNA).

## DISCUSSION

This study demonstrates an effective and simple method for the determination of murine NAT2 genotype and shows a clear association between genotype and phenotype. The use of probe substrates to define NAT isotype activity has been used in many previous studies for humans and mice [1]. The compound *p*ABA is a recognised specific substrate for both human NAT1 and mouse NAT2. The folate catabolite *p*AB-Glu has been demonstrated to be a substrate for human NAT1 [21, 28]. This report provides supporting evidence that *p*AB-Glu is also a substrate for mouse NAT2, an observation recently made by others studying recombinant enzymes [24]. A scheme of folate metabolism (based on [32]), on which the role of NAT in acetylation of *p*AB-Glu is superimposed, can be seen in Fig. 5.

The tissue distribution for murine NAT2 specific activity was similar for both *p*ABA and *p*AB-Glu as substrates investigated with spleen, liver, and kidney from C57BL/6J mice. The differences in *p*ABA and *p*AB-Glu acetylation activities observed between the fast and slow mouse strains in this study (Fig. 3) is at the high end of the ranges which have been observed previously [25, 26], but is within the threefold range predicted for liver NAT activity from *in*

*vivo* studies [39]. The heart and the two regions of the brain investigated demonstrated less difference between the fast and slow acetylating mouse strains with *p*ABA and *p*AB-Glu (Fig. 3, a and b). Previous studies have indicated the presence of murine NAT in the brain [25, 36]. The demonstration of mouse NAT2 activity in the cytosol of the cerebellum agrees with earlier immunohistochemical observations that there is NAT2 in specific neurones within the brain, including the Purkinje cells of the cerebellum [36]. The same cellular distribution of NAT in rate cerebellum has also been demonstrated using *in situ* hybridisation [40]. It may be significant that the tissues which show less of a difference between the two species of mice are those in which murine NAT2 is expressed earliest in embryonic development, namely the heart and neural tissues, Fig. 3 and [36].

Our results support the suggestion that murine NAT2, like human NAT1, could be involved in folate catabolism (Fig. 5). We have observed previously that murine NAT2 is expressed in the neural tube of developing embryos and show here clear evidence that the gene is transcribed in preimplantation embryonic stem cells (Fig. 4). The acetylated form of *p*AB-Glu is a major excretory product from the folate cycle (Fig. 5). Factors affecting the acetylation of *p*AB-Glu might be expected to influence this cycle. Previous studies have implied a link between acetylation and susceptibility to NTD. Differences in the incidence of cleft lip and cleft lip and palate have been linked to the acetylator locus in congenic mouse strains [34, 35]. The incidence of these congenital defects associated with anterior neural tube closure increases after the addition of the androgen glucocorticoid [41]. A recent study has demonstrated the presence of a hormone response element upstream of murine NAT2 sensitive to glucocorticoid [42]. Others have observed increased *N*-acetylation in the presence of glucocorticoid in rats [43] and rabbits [44]. These observations forge a link between glucocorticoid administration, murine NAT2 expression, and congenital defects in mice.

Genetic disorders such as mutations in 5,10-methylenetetrahydrofolate reductase (MTHFR) [45], a deficiency in dietary folate, or an imbalance in the removal of folate catabolites could upset the finely tuned folate cycle. Mutations within the MTHFR gene account for approximately 13% of NTDs in humans [46]. However, folate supplementation can result in a 70% decrease in NTDs [33]. Therefore, additional factors must be involved in dysfunction of the folate cycle and defective pyrimidine biosynthesis has been proposed as one factor [47]. We suggest that acetylation polymorphisms at the murine NAT2, or human NAT1, locus should also be considered as a candidate factor. The observation that murine NAT2 is transcribed in preimplantation embryonic stem cells, prior to neurulation, strengthens the case for investigation of NAT in relation to defects of neural tube closure in which folate has a protective role.



- phism of the human arylamine N-acetyltransferase type 1 gene caused by (CT)-T-190 and G(560)A mutations. *Pharmacogenetics* **8**: 67–72, 1998.
11. Grant DM, Hughes NC, Janezic SA, Goodfellow GH, Chen HJ, Gaedigk A, Yu VL and Grewal R, Human acetyltransferase polymorphisms. *Mutat Res* **376**: 61–70, 1997.
  12. Payton MA and Sim E, Genotyping human arylamine N-acetyltransferase type 1 (NAT1): The identification of a novel mutation. *Biochem Pharmacol* **55**: 361–366, 1998.
  13. Vatsis KP, Weber WW, Bell DA, Dupret JM, Evans DA, Grant DM, Hein DW, Lin HJ, Meyer UA, Relling MV, Sim E, Susuki T and Yamazoe Y, Nomenclature for N-acetyltransferases. *Pharmacogenetics* **5**: 1–17, 1995.
  14. Cartwright RA, Glashan RW, Rogers HJ, Ahmad RA, Barham-Hall D, Higgins E and Kahn MA, Role of N-acetyltransferase phenotypes in bladder carcinogenesis: A pharmacogenetic epidemiological approach to bladder cancer. *Lancet* **16**: 842–845, 1982.
  15. Risch A, Wallace DM, Bathers S and Sim E, Slow N-acetylation genotype is a susceptibility factor in occupational and smoking related bladder cancer. *Hum Mol Genet* **4**: 231–236, 1995.
  16. Bell DA, Stephens EA, Castranio T, Umbach DM, Watson M, Deakin M, Elder J, Hendrickse C, Duncan H and Strange RC, Polyadenylation polymorphism in the acetyltransferase 1 gene (NAT1) increases risk of colorectal cancer. *Cancer Res* **55**: 3537–3542, 1995.
  17. Probst-Hensch NM, Haile RW, Li DS, Sakamoto GT, Louie AD, Lin BK, Frankl HD, Lee ER and Lin HJ, Lack of association between the polyadenylation polymorphism in the NAT1 (acetyltransferase 1) gene and colorectal adenomas. *Carcinogenesis* **17**: 2125–2129, 1996.
  18. Levy G and Weber W, 2-Aminofluorene-DNA adduct formation in acetylator congenic mouse strains. *Carcinogenesis* **10**: 705–709, 1989.
  19. Cribb AE, Nakamura H, Grant DM, Miller MA and Spielberg SP, Role of polymorphic and monomorphic human arylamine N-acetyltransferases in determining sulfamethoxazole metabolism. *Biochem Pharmacol* **45**: 1277–1282, 1993.
  20. Palamanda J, Hickman D, Ward A, Sim E, Romkes-Sparks M and Unadkat J, Dapsone acetylation by human liver N-acetyltransferase and interaction with antiopportunistic infection drugs. *Drug Metab Dispos* **23**: 473–477, 1995.
  21. Minchin RF, Acetylation of para-aminobenzoylglutamate, a folate catabolite, by recombinant human NAT and U937 cells. *Biochem J* **307**: 1–3, 1995.
  22. Evans DAP, Manley KA and McKusick VA, Genetic control of isoniazid acetylation in man. *Br Med J* **2**: 485–491, 1960.
  23. Tannen R and Weber W, Inheritance of acetylator phenotype in mice. *J Pharmacol Exp Ther* **213**: 480–484, 1980.
  24. Estrada-Rodgers L, Levy G and Weber W, Substrate selectivity of mouse N-acetyltransferases 1, 2 and 3 expressed in Cos-1 cells. *Drug Metab Dispos* **26**: 502–505, 1998.
  25. Chung J, Levy G and Weber W, Distribution of 2-aminofluorene and p-aminobenzoic acid N-acetyltransferase activity in tissues of C57BL/6J rapid and B6.A-Nats slow acetylator congenic mice. *Drug Metab Dispos* **21**: 1057–1063, 1993.
  26. Stanley L, Mills I and Sim E, Localisation of polymorphic N-acetyltransferase (NAT2) in tissues of inbred mice. *Pharmacogenetics* **7**: 121–130, 1997.
  27. Fretland A, Doll M, Gray K, Feng Y and Hein D, Cloning, sequencing, and recombinant expression of NAT1, NAT2, and NAT3 derived from C3H/HeJ (rapid) and A/HeJ (slow) acetylator inbred mouse: Functional characterisation of the activation and deactivation of aromatic carcinogens. *Toxicol Appl Pharmacol* **142**: 360–366, 1997.
  28. Ward A, Summers M and Sim E, Purification of recombinant human NAT1 expressed in *E. coli*. *Biochem Pharm* **49**: 1759–1767, 1995.
  29. Pheasant A, Blair J, Saleh A, Guest A, Barford P, Choolun R and Allan R, Possible mechanisms of folate breakdown. In: *Chemistry and Biology of Pteridines* (Ed. Blair J), pp. 1007–1012. Walter de Gruyter & Co., Berlin, New York, 1983.
  30. Murphy M and Scott J, The turnover, catabolism and excretion of folate administered at physiological concentrations in the rat. *Biochim Biophys Acta* **583**: 535–539, 1979.
  31. McNulty H, McPartlin J, Weir D and Scott J, Folate catabolism is increased during pregnancy in rats. *J Nutr* **123**: 1089–1093, 1993.
  32. Scott JM, Weir DG, Molloy A, McPartlin J, Daly L and Kirke P, Folic acid metabolism and mechanisms of neural tube defects. *Ciba Found Symp* **181**: 180–187, 1994.
  33. MRC Vitamin Study Research Group, Prevention of neural tube defects: Results of the MRC vitamin study. *Lancet* **338**: 131–137, 1991.
  34. Karolyi J, Erickson RP, Liu S and Killewald L, Major effects on teratogen-induced facial clefting in mice determined by a single genetic region. *Genetics* **126**: 201–205, 1990.
  35. Karyoli J, Liu S and Erickson R, Susceptibility to phenytoin-induced cleft lip with or without cleft palate: Many genes are involved. *Genet Res* **49**: 43–49, 1987.
  36. Stanley L, Copp A, Pope J, Rolls S, Smelt V, Perry VH and Sim E, Immunochemical detection of arylamine N-acetyltransferase during mouse embryonic development and in adult mouse brain. *Teratology* **58**: 174–182, 1998.
  37. Nakajima-Iijima S, Hamada H, Reddy P and Kakunaga T, Molecular structure of the human cytoplasmic beta-actin gene: Interspecies homology of sequences in the introns. *Proc Natl Acad Sci USA* **82**: 6133–6137, 1985.
  38. Ward A, Hickman D, Gordon JW and Sim E, Arylamine N-acetyltransferase in human red blood cells. *Biochem Pharmacol* **44**: 1099–1104, 1992.
  39. Hultin T and Weber W, Genetic differences in 2-aminofluorene pharmacokinetics between intact C57BL/6J and A/J mice. *Drug Metab Dispos* **13**: 148–150, 1985.
  40. King CM, Land SJ, Jones RF, Debiec-Rychter M, Lee MS and Wang CY, Role of acetyltransferases in the metabolism and carcinogenicity of aromatic amines. *Mutat Res* **12**: 123–128, 1997.
  41. Liu S and Erickson R, Genetic differences among the A/J × C57BL/6J recombinant inbred mouse lines and their degree of association with glucocorticoid-induced cleft palate. *Genetics* **113**: 745–754, 1986.
  42. Estrada-Rodgers L, Levy G and Weber W, Characterisation of a hormone response element in the mouse N-acetyltransferase 2 (Nat2\*) promoter. *Gene Exp* **7**: 13–24, 1998.
  43. Zaher H and Svensson C, Glucocorticoid induction of hepatic acetyl CoA: arylamine N-acetyltransferase activity in the rat. *Res Commun Chem Pathol Pharmacol* **83**: 195–208, 1994.
  44. Reeves P, Minchin R and Ilett K, *In vivo* mechanisms for the enhanced acetylation of sulphamethazine in the rabbit after hydrocortisone treatment. *J Pharmacol Exp Ther* **248**: 348–352, 1989.
  45. Mudd S, Uhlenhuth B, Freeman J, Finkelstein J and Shih V, Homocystinuria associated with decreased methylenetetrahydrofolate reductase activity. *Biochem Biophys Res Commun* **46**: 905–912, 1972.
  46. Posey D, Khourney M, Mulinare J, Adams M and Ou C, Is mutated MFTHR a risk factor for neural tube defects? *Lancet* **347**: 686–687, 1996.
  47. Fleming A and Copp A, Embryonic folate metabolism and mouse neural tube defects. *Science* **280**: 2107–2109, 1998.